AD-A030786

MS-R-7704

AN APPROACH TO THE LIMITED APERTURE PROBLEM OF PHYSICAL OPTICS FARFIELD INVERSE SCATTERING

by

Robert D. Mager† and Norman Bleistein
Mathematics Department, College of Arts & Sciences
and
Mathematics Division, Denver Research Institute
University of Denver

Reproduced by NATIONAL TECHNICAL INFORMATION SERVICE
U.S. Department of Commerce
Springfield, VA 22151

This research was supported by the Office of Naval Research.

†Present address: Mathematics Department
Colorado School of Mines
Golden, Colorado 80401

DDC
OCT 14 1976

Abstract

We examine the limited aperture problem of physical optics farfield inverse scattering, i.e., the problem of identifying a target from an analysis of band-limited viewing apertures. We show (given information from all directions) that the target may be completely identified from an analysis of high frequency, band-limited data. If the directions of viewing angles are limited as well, it is shown that the target surface can be identified where the target normal lies within the range of viewing directions; outside of this range, no information is available. It is shown that this phenomenon is totally a feature of the Fourier transform of characteristic (non-zero) functions and independent of the inverse scattering formalism. Numerical examples are given for the case of a perfectly reflecting circular cylinder

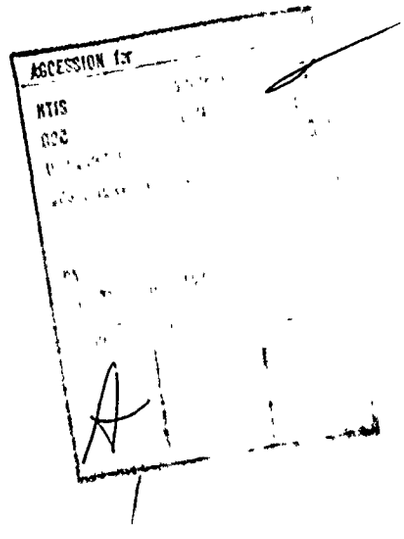

1. Introduction.

Physical optics inverse scattering constitutes a technique whereby the shape and location of an acoustical or electromagnetic scattering target may be determined from an analysis of back-scattered, far-field data. The fundamental identity of the method (first discovered by Bojarski, [1]) relates a quantity $\rho_{\pm}(\underline{\kappa})$ (that is proportional to the back-scattering cross-section of radar analysis), to the Fourier transform of the characteristic function of the scattering target; i.e., a function which is unity inside the target, and zero outside.

The key assumptions leading to the Bojarski identity are (1) that the target may be modelled as an acoustically hard or soft reflector (or as a perfect conductor in the electromagnetic case); (2) that the physical optics approximation is valid for the back-scattered fields; and (3) that the source and observation ranges are large compared to a typical target dimension. The fundamental identity*, which is derived briefly in Appendix A for the reduced wave equation, states that

$$\tilde{\Gamma}(\underline{\kappa}) = \frac{\rho_{+}(\underline{\kappa}) + \rho_{-}^{*}(-\underline{\kappa})}{\kappa^2} \quad , \tag{1.1}$$

where $\Gamma(\underline{X})$ is the target characteristic function, and $\tilde{\Gamma}(\underline{\kappa})$ is its Fourier transform. In this expression, the transform vector $\underline{\kappa}$ is given by

$$\underline{\kappa} = 2k\hat{\underline{X}} \qquad k = \frac{\omega}{c} \, , \tag{1.2}$$

*Below, we shall use the alliteration POFFIS for "Physical Optics Farfield Inverse Scattering".

where k is the wave propagation number, ω is the (time-harmonic) frequency, and c is the propagation speed; the vector $\hat{X}$ is a unit vector pointing in the direction of the source-observation position. The symbol (*) denotes complex conjugation.

Therefore, if $\tilde{\Gamma}(\underline{\kappa})$ could be measured for a sufficiently large class of vectors $\underline{\kappa}$, one could in principal determine $\Gamma(\underline{X})$ by direct Fourier inversion. As (1.2)clearly implies, this would necessitate that measurements be performed at all frequencies and at all aspect angles with respect to the target about which information is desired.

An immediate difficulty which arises with the method, therefore, is the lack of complete information in transform space; the physical optics approximation is valid only in the high-frequency regime, i.e., as the wavenumber k approaches infinity. Furthermore, data that would be available from an actual experiment would most likely be confined to some band-limited spectrum. A further limitation of the POFFIS method occurs because data can seldom be measured at all aspect-angles with respect to the unknown target.

These difficulties lead to the *limited-aperture* problem of the POFFIS method -- the problem of identifying the target structure from the limited knowledge of $\hat{\Gamma}(\underline{\kappa})$ in $\underline{\kappa}$-space. The objective of this paper is to present solutions to the limited-aperture problem for a physically reasonable class of frequency and aspect-angles limited apertures.

We show (given information from all directions) that the target may be completely identified from an analysis of high-frequency, band-limited data. If the aperture is limited in aspect angles as well, it will be shown that the target surface can be unambiguously determined at those points where the outward normal to the target surface lies within the range of directions defined by the aperture in $\underline{\kappa}$-space. Outside of this range, no information is possible by this method.

The limited-aperture problem has been previously examined (from an analytical standpoint) by Lewis [2] and Perry [3]. Lewis considered a number of aspect-angles limited apertures, with the (physically unreasonable) assumption that information was available for all frequencies. Perry concluded that the absence of low-frequency information leads to an ill-posed problem which is numerically unstable. The primary difficulty is that the low-frequency data constitutes a principal contribution to the gross resolution of the function $\Gamma(\underline{X})$.

Additional tests of Bojarski's results were carried out numerically in papers by Tabbara [4, 5] and Rosenbaum-Raz [6]. Their results confirm the difficulties with resolution due to bandlimiting. One purpose of this paper is to show how this shortcoming of the method can be overcome.

The key feature of the method we describe here is that we replace the problem of determining $\Gamma(\underline{X})$ by the problem of determining the *directional derivative* of $\Gamma(\underline{X})$ in some direction $\hat{\xi}$. The directional derivative $\hat{\xi} \cdot \nabla\Gamma(\underline{X})$ is a highly singular function whose essential features can be resolved from an analysis of high-frequency data. The process of differentiating in the $\hat{\xi}$ direction

in $\underline{X}$-space corresponds to multiplication by $\hat{\xi} \cdot \underline{\kappa}$ in $\underline{\kappa}$-space; in this way, one simultaneously suppresses low-frequency data while enhancing high-frequency data.* Indeed, this approach was first suggested in Bojarski's initial work [1], and the present work supports and extends his ideas.

In section (2) are displayed a number of computer-generated examples for a variety of limited-data apertures. These examples were generated from the *exact* back-scattered, far-field data which was numerically computed according to a scheme by Greenspan and Werner [7].

We remark that the advantage gained by calculating the Fourier transform of a directional derivative is wholly a feature of Fourier analysis. It has nothing to do with Bojarski's physical optics identity, nor has it anything to do with the discretization and specific calculation technique (FFT in this work) used in the inversion of the transform. It is shown in Section 3 by asymptotic methods why the band-limited transform behaves as it does.

More precisely, in two dimensions, we express the band-limited inverse Fourier transform of the directional derivative as a threefold integral in arc length over the boundary of the target, and κ and θ, the magnitude and angle of the transform vector $\underline{\kappa}$. Under the assumption of high frequency band-limiting, the first and third of these integrals can be calculated asymptotically by the method of two-dimensional stationary phase [8]. The integration in magnitude $\underline{\kappa}$ is carried out exactly. The result of this calculation explains the qualitative features of the numerical results

*Multiplication by higher powers of κ, correspond to higher derivatives, further subdues the effect of low frequence data and further enhances the effect of high frequency data.

shown in Section (2). Furthermore, stationary phase analysis brings out the features of the aspect-angles problem, as well; namely, given a certain range of aspect angles in transform space, the inverse transform is asymptotically of lower order outside of the analogous aperture in physical space.

The extension of this analysis to the case of three dimensions is discussed in Appendix B.

2. Numerical Results

Figures (2.1-8) display the results of the method. They were generated in the following way. The reduced wave equation was solved for a point source in the exterior of a totally reflecting circular cylinder by a method due to Greenspan and Werner [7]. The phase and range normalized backscattered amplitude (defined below (A.11) in the Appendix) is calculated to five place accuracy. This is then substituted into Bojarski's basic identity (1.1) to yield $\hat{\Gamma}(\underline{\kappa})$. Table I compares the exact Fourier transform for the target cross-section with that predicted by the inverse diffraction technique. Agreement is poor for wave numbers below ka = 10, emphaizing the need for high frequency, band-limited analysis. We remark that the source-observation range was 25 radii, indeed in the far field, so that this could not have accounted for the discrepancy at moderate values of ka.

The backscattered data was used in the formula

$$\hat{\xi} \cdot \nabla \Gamma(\underline{X}) = (2\pi)^{-2} \int i\, \hat{\xi} \cdot \underline{\kappa}\, \hat{\Gamma}(\underline{\kappa})\, e^{i\underline{\kappa}\cdot\underline{X}}\, d\underline{\kappa} \quad , \tag{2.1}$$

for the directional derivative of the characteristic function. Here the domain of integration is all of κ-space. In particular, we chose

$$\hat{\xi} = (1,0) \quad , \tag{2.2}$$

corresponding to transverse differentiation of $\Gamma(\underline{X})$, an proceed to calculate (2.1) over finite domains representing band-limited and

aspected-angles limited apertures.

The inverse transform is calculated via a fast-Fourier transform (FFT) routine. Band-limited data around $k = 10$, 20 and was used, with a mesh size of 128×128 (of which most entries were zero) and mesh-widths $\Delta\kappa_1 = \Delta\kappa_2 = 1.1$. The resulting function was then computer-displayed to yield the graphical results shown in Figures (2.1-7).

The resolution in those diagrams is seen to be approximately one-half the minimum wavelength associated with the domain of integration in κ . The clarity of the results is also seen to be directly a function of the frequency band-width, as expected. Furthermore, we believe that better resolution may be attained by curve fitting the actual output to the results predicted by the asymptotic analysis in the next section. The "smearing" effect near the lower and upper portions of the target is due to the fact that we calculate the transverse derivative of $\Gamma(\underline{X})$, and this derivative approaches zero at these limits. This minor shortcoming maybe overcome in one of the following ways: (1) calculating a directional derivative which does not vanish in these limits (different $\hat{\xi}$) or (2) by calculating a higher derivative (for example, by multiplying by κ^2 rather than $\hat{\xi} \cdot \underline{\kappa}$ before inverting the Fourier transform).

Figures (3.5-7) show the results from a viewing aperture which is limited in direction, as well. The theory developed in the next section will predict good resolution of the target surface where the outward normal to the target lies within the family of directions

specified by the viewing aperture; outside of this range no information is available.

One further remark is due concerning the computer plotting results. The theory developed in the next section is based upon leading order asymptotic effects. There are also secondary effects, corresponding to boundary integral contributions, etc., but these do not appear due to normalization in the plotting process.

3. Limited Aperture Analysis

We proceed in this section with an analysis of the integral (2.1). Let us denote the region of $\underline{\kappa}$-space where the measured function $\hat{\Gamma}(\underline{\kappa})$ is known by D, and the characteristic function of D by $A(\underline{\kappa})$:

$$\tilde{A}(\underline{\kappa}) = \begin{cases} 1 & \underline{\kappa} \in D \\ 0 & \underline{\kappa} \notin D \end{cases}$$

We consider the function

$$\tilde{\Gamma}_1(\underline{\kappa}) = i\,\hat{\xi} \cdot \underline{\kappa}\,\hat{\Gamma}(\underline{\kappa}) \ . \tag{3.1}$$

This is the Fourier transform of the directional derivative of $\Gamma(\underline{X})$ in the $\hat{\xi}$ direction. We note that the product of $\Gamma_1(\underline{\kappa})$ and the aperture function $\hat{A}(\underline{\kappa})$,

$$\hat{H}(\underline{\kappa}, \hat{\xi}) = \tilde{A}(\kappa)\,\tilde{\Gamma}_1(\underline{\kappa}) \ , \tag{3.2}$$

is known everywhere in $\underline{\kappa}$-space. We consider first the two-dimensional version of (3.2) (Applicable when the target is known to be a cylinder whose cross-sectional profile is sought). We introduce as new coordinates arc length σ along the boundary curve ∂B and distance normal to the boundary, denoted by s (see Figure (3.1)). The directional derivative, $\Gamma_1(\underline{X})$, may be represented as

$$\Gamma_1(\underline{X}) = \hat{\xi} \cdot \nabla\,\Gamma(\underline{X}) = \hat{\xi} \cdot \hat{n}\,\delta(s) \ .$$

Here $\hat{n} = \hat{n}(\sigma)$ is the outward unit normal to ∂B. A Fourier inversion of (3.1) and use of the convolution theorem for Fourier

transforms leads to

$$H(\underline{X},\hat{\xi}) - (2\pi)^{-2} \int_{\partial B} \hat{n}(\sigma) \cdot \hat{\xi}\, A(\underline{X} - \underline{X}'(\sigma))d\sigma \qquad (3.3)$$

The objective of this analysis is to evaluate (3.3) asymptotically in the high frequency limit, i.e., for κ = target anywhere in $\mathcal{D}$. We use the explicit representation of $A(\underline{X})$,

$$A(\underline{X}) = \iint_D e^{i\underline{\kappa}\cdot\underline{X}}\, d\underline{\kappa} ,$$

to rewrite (3.3) as

$$H(\underline{\kappa},\hat{\xi}) = (2\pi)^{-2} \int_{\partial B} d\sigma\, \hat{n}(\sigma) \cdot \hat{\xi} \iint_D e^{i\underline{\kappa}\cdot(\underline{X}-\underline{X}'(\sigma))} d\underline{\kappa} \qquad (3.4)$$

The three-dimensional analogue of (3.4) is

$$H(\underline{X},\hat{\xi}) = (2\pi)^{-3} \int_{\partial B} d\underline{\sigma}\, \hat{n}(\underline{\sigma}) \cdot \hat{\xi} \iint_D d^{i\underline{\kappa}\cdot(\underline{X}-X'(\sigma))} d\underline{\kappa} , \qquad (3.5)$$

where $\underline{\sigma} = (\sigma_1,\sigma_2)$ represents surface coordinates over ∂B (Figure (3.2)). Analysis of (3.5) is carried out in Appendix B and we proceed with the analysis of (3.4) here.

Consider an aperture which is limited in both frequency and directions, as illustrated in Figure (3.3); note that the $\underline{\kappa}$-space aperture D must be symmetric about the origin by virtue of the analysis leading to the physical optics identity (Appendix A, equation (A.13)). (When the aperture directions are restricted to one-sided viewing, it is possible to extend the data symmetrically through the origin in $\underline{\kappa}$-space; the reconstructed image will then be symmetric in physical space (Lewis [2]), and one has no information concerning the opposite side of the target.)

Define $\underline{\kappa} = \kappa\hat{\kappa}$, where κ and $\hat{\kappa}$ are the magnitude and directions of $\underline{\kappa}$, and rewrite (3.4) as

(3.6)

$$H(\underline{X},\hat{\xi}) = \left(\frac{1}{2\pi}\right)^2 \int_{\kappa_0}^{\kappa_1} \kappa d\kappa \int_{\partial B} d\sigma \hat{n}(\sigma) \cdot \hat{\xi} \int_{\Omega D} e^{i\kappa\hat{\kappa}(\theta) \cdot (\underline{X} - \underline{X}'(\sigma))} d\theta \ ;$$

the angular integration in this expression is described by the parameter θ, which is taken to be the angle of the vector $\hat{\kappa}$.

With the assumption that $\kappa_0 >> 1$, the expression in (3.6) may be examined via a stationary phase analysis in the variables (σ,θ). With the phase function $\Phi(\sigma,\theta)$ defined by

$$\Phi(\sigma,\theta) = \hat{\kappa}(\theta) \cdot (\underline{X} - \underline{X}'(\sigma)) \quad ,$$

the stationary phase conditions become

$$\Phi_\sigma = -\hat{\kappa}(\theta) \cdot \underline{T}(\sigma) = 0 \ , \quad \underline{T} = \frac{d\underline{X}(\sigma)}{d\sigma} \ , \tag{3.7}$$

$$\Phi_\theta = \hat{\tau}(\theta) \cdot (\underline{X} - \underline{X}'(\sigma)) = 0 \ , \quad \hat{\tau}(\theta) = \frac{d\hat{\kappa}(\theta)}{d\sigma} \ . \tag{3.8}$$

Let Σ represent the portion of the surface ∂B where the family of normals $\hat{n}(\sigma)$ lie within the range of directions specified by the aperture D. Then the conditions (3.7) and (3.8) will be satisfied in Σ when the vector $\underline{X} - \underline{X}'(\sigma)$ is orthogonal to the tangent vector $\underline{T}$ to ∂B, and when $\hat{\kappa}(\theta)$ is collinear with $\underline{X} - \underline{X}'(\sigma)$, as illustrated in figure (3.4).

Since the $\underline{\kappa}$-space aperture is symmetric about the origin, there exist two solutions, $\theta = \theta_\pm$, for which

$$\hat{\kappa}(\theta_+) = -\hat{\kappa}(\theta_-) \ . \tag{3.9}$$

There may also exist a multiple of solutions in the arc-length variable σ; however, it will be evident from further analysis

that the stationary point $\sigma = \sigma_m$ for which $(\underline{X} - \underline{X}'(\sigma))$ is a minimum will dominate.

Define the two-dimensional Hessian matrix H_e by

$$H_e = \det[\Phi(\sigma,\theta)] \ ;$$

we note that

$$H_e = -|\underline{X} - \underline{X}'(\sigma_m)|\chi C_0 - \left|\frac{d\underline{X}'(\sigma_m)}{d\sigma}\right|^2$$

In this expression, $\chi = \chi(\sigma_m)$ is the curvature of the target surface ∂B at $\sigma = \sigma_m$, and

$$C_0 = \begin{cases} +1 & \underline{X} \in B \\ -1 & \underline{X} \notin B \end{cases}$$

With these identifications, $H(\underline{X},\hat{\xi})$ is asymptotically equal to

$$H(\underline{X},\hat{\xi}) \sim \left(\frac{1}{\pi}\right) \int_{\kappa_0}^{\kappa_1} d\kappa \hat{n}(\sigma_m) \cdot \hat{\xi} \, \frac{\mathrm{Cos}\left\{\kappa|\underline{X} - \underline{X}'(\sigma_m)|\right\}}{\sqrt{|\det(H_e)}} \ ;$$

that is,

$$H(\underline{X},\hat{\xi}) \sim \frac{\hat{n}(\sigma_m) \cdot \hat{\xi}}{\pi\sqrt{|\det(H_e)}} \left\{ \frac{\mathrm{Sin}(\kappa_1|\underline{X} - \underline{X}'(\sigma_m)|) - \mathrm{Sin}(\kappa_0|\underline{X} - \underline{X}'(\sigma_m)|)}{|\underline{X} - \underline{X}'(\sigma_m)|} \right\} \quad (3.10)$$

The function $H(\underline{X},\hat{\xi})$ thus behaves in the region Σ (and in the high-frequency limit) as a SinX/X function with central lobe located on the target surface; a trace of $H(\underline{k},\hat{\xi})$ would therefore yield information about the unknown target in the region Σ.

This analysis is not valid when the Hessian matrix H_e becomes singular; the vanishing of $\det(H_e)$ occurs on the evolute of the target

surface ∂B. These are stationary points of higher order. However, one can verify that the amplitude at those points is zero and hence the contribution from such a stationary point is lower order than the contributions derived above.

The calculations leading to (3.10) have been concerned with an estimate of contributions arising from stationary points *interior* to the boundary of the $\sigma - \Theta$ domain of integration, labeled as $\partial(D,B)$ in Figure (3.5). (Note that $D = S_1 + S_2 + \ldots + S_8$.

In general, contributions from stationary points on the boundary surface $\partial(D,B)$ will also occur. Define the vector $\underline{U}$ by

$$\underline{U} = \frac{\nabla\Phi}{|\nabla\Phi|^2} , \qquad \nabla = \left(\frac{\partial}{\partial\sigma} , \frac{\partial}{\partial\Theta}\right) , \tag{3.11}$$

and note that

$$ge^{i\kappa\Phi} = \frac{ie^{i\kappa\Phi}}{\kappa} \nabla \cdot \underline{U} - \frac{i}{\kappa} \nabla \cdot (\underline{U}e^{i\kappa\Phi}) .$$

Then to leading order,

$$H(\underline{X},\hat{\xi}) \sim \frac{e^{-i\pi/2}}{(2\pi)^2} \int_{\kappa_0}^{\kappa_1} d\kappa \int_{\partial(D,B)} (\hat{n}(\sigma) \cdot \hat{\xi})(\hat{N} \cdot \underline{U}) We^{i\kappa\hat{\kappa}(\Theta) \cdot (\underline{X} - \underline{X}'(\sigma))} d\sigma \tag{3.12}$$

where α describes the one-parameter surface $\partial(B,\Omega_k)$,

$$\Theta = \Theta(\alpha) , \qquad \sigma = \sigma(\alpha) ,$$

and

$$W = \sqrt{J^T J} , \qquad J = \begin{pmatrix} \Theta_\alpha \\ \sigma_\alpha \end{pmatrix} .$$

The unit vector $\hat{N} = \hat{N}(\alpha)$ points to the exterior of $\partial(D,B)$. A stationary phase analysis may now be performed on the remaining α-integral in (3.12); these points of stationarity will yield the $\partial(D,B)$ boundary contributions. The objective in considering these *lower order* contributions is to show that no information is forthcoming concerning those points in Σ on ∂B whose outward normals lie outside of the set of directions implied by the $\underline{\kappa}$-space aperture D; outside of Σ, no *interior* stationary points exist and the boundary terms play the dominant role.

We begin by considering the contributions from boundaries S_5 and S_7; a similar analysis will yield corresponding results for boundaries S_6 and S_8. Furthermore, the total contribution from $S_1 - S_4$ can be seen by similar methods to vanish to leading asymptotic order.

On the boundary S_5, the following identifications can be made:

$$\Theta = \phi_0 \qquad \alpha = \sigma$$

$$\Rightarrow J = \begin{pmatrix} 0 \\ 1 \end{pmatrix} \Rightarrow W = 1$$

$$\hat{N} = (0,-1)$$

Equation (3.12) then assumes the form

$$H(\underline{X},\hat{\xi}) \sim \frac{e^{-i\pi/2}}{(2\pi)^2} \int_{\kappa_0}^{\kappa_1} d\kappa \int_{\sigma_i}^{\sigma_T} (\hat{n} \cdot \hat{\xi})(\hat{N} \cdot \underline{U}) e^{i\kappa\hat{\phi}(\phi_0) \cdot (\underline{X} - \underline{X}'(\sigma))} d\sigma.$$

Identify the phase function Φ_5 as

$$\Phi_5 = \hat{\kappa}(\phi_0) \cdot (\underline{X} - \underline{X}'(\sigma));$$

then the condition of stationary phase becomes

$$\frac{d\Phi_5}{d\sigma} = -\hat{\kappa}(\phi_0) \cdot \underline{T}(\sigma) = 0 \ , \quad \underline{T} = \frac{d\underline{X}(\sigma)}{d\sigma} \ . \qquad (.13)$$

Condition (3.13) has at least one solution $\sigma = \sigma_5$, where

$$\hat{\kappa}(\phi_0) \perp \underline{T}(\sigma_5).$$

The factor $\hat{N} \cdot \underline{U}$ then has the explicit form

$$\hat{N} \cdot \underline{U} = \frac{-\hat{\tau}(\phi_0) \cdot (\underline{X} - \underline{X}'(\sigma_5))}{\left[(\hat{\tau}(\phi_0) \cdot (\underline{X} - \underline{X}'(\sigma_5))\right]^2} \ , \quad \hat{\tau} = \frac{d\hat{\kappa}(\theta)}{d\theta} \ .$$

Note further that

$$\frac{d^2\Phi_5}{d\sigma^2} = -\hat{\kappa}(\phi_0) \cdot \frac{d\underline{T}(\sigma_5)}{d\sigma} = +\chi(\sigma_5),$$

where $\chi(\sigma_5)$ again represents curvature at the point $\sigma = \sigma_5$; for a convex body, this quantity is positive. A one-dimensional stationary phase calculation therefore gives

$$H_5(\underline{X}, \hat{\xi}) \sim \frac{e^{-i\pi/2}}{(\chi(\sigma_5))^{1/2}(2\pi)^{3/2}} \int_{\kappa_0}^{\kappa_1} \frac{d\kappa}{\kappa^{1/2}} (\hat{n}(\sigma_5) \cdot \hat{\xi})$$

$$(\hat{N}_5 \cdot \underline{U}) e^{i\{\kappa\hat{\kappa}(\phi_0) \cdot (\underline{X} - \underline{X}'(\sigma_5)) + \pi/4\}} \ ,$$

where $\hat{N}_5$ is to outward normal in $(\sigma - \theta)$ space to S_5.

An analysis of the boundary S_7 (where $\theta = \pi + \phi_0$) will yield a similar result, with a stationary solution in σ again at $\sigma = \sigma_5$;

the only distinction in this case is that now

$$\hat{\kappa}(\pi + \phi_0) = -\hat{\kappa}(\phi_0)$$

and

$$(\hat{N}_5 \cdot \underline{U}) \Big|_{\Theta = \phi_0} = -(\hat{N}_7 \cdot \underline{U}) \Big|_{\Theta = \pi + \phi_0}$$

The sum of the leading order contributions from s_5 and s_7, therefore, gives

$$H_{5+7}(\underline{X}, \hat{\xi}) \sim \frac{(\hat{n}(\sigma_5) \cdot \hat{\xi})(\hat{N}_5 \cdot \underline{U}(\phi_0))}{(\chi(\sigma_5))^{1/2}(2\pi)^{3/2}}$$

$$\int_{\kappa_0}^{\kappa_1} \frac{\mathrm{Sin}\{\kappa\hat{\kappa}(\phi_0) \cdot (\underline{X} - \underline{X}'(\sigma_5)) + \pi/4\}}{\kappa^{1/2}}\, d\kappa,$$

and by integration by parts (retaining only the leading order term)

$$H_{5+7}(\underline{X}, \hat{\xi}) \sim -\frac{(\hat{n}(\sigma_5) \cdot \hat{\xi})(\hat{N}_5 \cdot \underline{U}(\phi_0)}{(\chi(\sigma_5))^{1/2}(2\pi)^{3/2}}$$

$$\times \frac{\mathrm{Cos}\{\kappa\hat{\kappa}(\phi_0) \cdot (\underline{X} - \underline{X}'(\sigma_5)) + \pi/4\}}{\kappa^{1/2}\hat{\kappa}(\phi_0) \cdot (\underline{X} - \underline{X}'(\sigma_5))} \Bigg|_{\kappa_0}^{\kappa_1} \qquad (3.14)$$

The principal point to be concluded from an examination of (3.14) is that (in the exterior of the region Σ as identified in Figure (2.2)) $H(\underline{\kappa}, \hat{\xi})$ exhibits to leading order a peaking behavior with central lobe occurring in the vicinity of the line

$$\hat{\kappa}(\phi_0) \cdot (\underline{X} - \underline{X}'(\sigma_5) = 0 \ ,$$

where

$$\hat{\kappa}(\phi_0) \cdot \underline{T}(\sigma_5) = 0 \ ;$$

however, $H(\underline{X}, \hat{\xi})$ gives no information concerning the target surface in this region.

Appendix A.

In this section, we present a brief derivation of the POFFIS identity for acoustical wave propagation; the electromagnetic (vector) case has been outlined by Lewis [3].

As indicated in figure (A.1), we illuminate the acoustically hard or soft scatterer B from a time-harmonic point source located at $\underline{X}_0$. The incident field U_I is thus given by

$$U_I(\underline{X},k) = \frac{e^{ik|\underline{X} - \underline{X}_0|}}{4\pi|\underline{X} - \underline{X}_0|} \quad , \tag{A.1}$$

and the total acoustic field U_T is the sum of the incident U_I and a back-scattered field U_S, which is also measured at the point $\underline{X}_0$:

$$U_T = U_I + U_S \quad . \tag{A.2}$$

The total acoustic field U_T is required to satisfy the (time-reduced) acoustic wave equation with source at $\underline{X} = \underline{X}_0$:

$$(\nabla^2 + k^2)U_T = -\delta(\underline{X} - \underline{X}_0) \quad . \tag{A.3}$$

In addition, we require that U_T satisfy an outgoing radiation condition at infinity, and one of the two boundary conditions

$$\frac{\partial U_T}{\partial n} = 0 \qquad \underline{X} \in B \quad (+) \quad , \tag{A.4}$$

or

$$U_T = 0 \qquad \underline{X} \in B \quad (-) \; . \tag{A.5}$$

The first (+) boundary condition models B as an acoustically hard reflector; the second (-) condition is the acoustically soft case. Using (A.1) - (A.5) and the requirement that U_S also be outgoing at infinity, one may write a Kirchoff integral expression for U_S :

$$U_S(\underline{X}_0,k) = \iint_{\partial B} \left\{ U_S(\underline{X}',k) \frac{\partial G(\underline{X}_0 - \underline{X}')}{\partial n'} - G(\underline{X}_0 - \underline{X}') \frac{\partial U_S(\underline{X}',k)}{\partial n'} \right\} dS' \; , \tag{A.6}$$

where the integration is performed over the surface (denoted ∂B) of the scatterer B . In this expression, $G(\underline{X})$ is the free-space outgoing Green's function given by

$$G(\underline{X}) = \frac{e^{ik|\underline{X}|}}{4\pi|\underline{X}|} \; . \tag{A.7}$$

We now make a crucial assumption concerning the integrand of (A.6). Under the integration sign appear the unknown surface field U_S and the normal derivative $\frac{\partial U_S}{\partial n}$. The *physical optics* approximation relates U_S and $\frac{\partial U_S}{\partial n}$ to the incident field U_I on the surface of the scatterer by

$$\left.\begin{aligned} U_S &\sim \pm U_I \\ \frac{\partial U_S}{\partial n} &\sim \mp \frac{\partial U_I}{\partial n} \end{aligned}\right\} \quad \underline{X} \in L$$

$$\left. U_S = \frac{\partial U_S}{\partial n} = 0 \right\} \quad \underline{X} \in D \; , \tag{A.8}$$

where the (±) notation has the same connotation as before. We define the lit side of the body (denoted L) and the dark side (D) by constructing tangential rays from source to target, as indicated in figure (A.2). The envelope of the set of points where the rays strike the body will in general define a closed curve Σ separating the body into lit and dark sides.

Strictly speaking, (A.8) constitutes a valid identification only for the case of plane-wave incidence against a plane-wave reflector and in all other cases constitutes an approximation. But the approximation is increasingly valid for small wavelength (large k) propagation, where locally the indicent wavefront and the target surface may be approximated by their tangent planes [9]. The separation of the surface ∂B into a lit and a dark side also is strictly valid only for convex scatterers.

We may now use (A.8) to rewrite (A.6) as

$$U_S(\underline{X}_0,k) \sim \pm \iint_L \frac{\partial}{\partial n'} \left(U_S(X',k) G(\underline{X}_0 - \underline{X}') \right) dS' \ . \qquad (A.9)$$

Into this result, we now introduce the far-field approximations. Under the assumption that $|X_0| \gg |\underline{X}'|$ (distance to the source-receiver point is large compared to a typical target dimension), we write $|\underline{X}_0 - \underline{X}'|$ as two terms in a binomial series:

$$|\underline{X}_0 - \underline{X}'| \sim X_0 - \hat{X}_0 \cdot \underline{X}' \ , \qquad (A.10)$$

where $X_0 = |\underline{X}_0|$, and $\hat{X}_0$ represents a unit vector in the direction of $\underline{X}_0$. With these identifications, we have

$$U_I(\underline{X}',k) \sim \frac{e^{ik(X_0 - \hat{X}_0 \cdot \underline{X}')}}{4\pi X_0}$$

$$G(\underline{X}_0 - \underline{X}') \sim \frac{e^{ik(X_0 - \hat{X}_0 \cdot \underline{X}')}}{4\pi X_0}$$

and equation (A.9) becomes

$$U_S(\underline{X},k) \sim \pm \frac{e^{i2kX_0}}{(4\pi X_0)^2} \iint_L \frac{\partial}{\partial n'} \left\{ e^{-i2k\hat{X}_0 \cdot \underline{X}'} \right\} dS' \ .$$

We may now perform the normal differentiation to obtain

$$U_S(\underline{X},k) \sim \mp \frac{(2ik)e^{i2kX_0}}{(4\pi X_0)^2} \iint_L \hat{n} \cdot \hat{X}_0 e^{-i2k\hat{X}_0 \cdot \underline{X}'} dS' \ , \qquad (A.11)$$

Defining the phase and range normalized backscattered field $\rho_+(\underline{X}_0,k)$ by

$$U_S(\underline{X}_0,k) = \frac{e^{i2kX_0}}{(4\pi X_0)^2} \rho_+(\underline{X}_0,k) \ ,$$

then (A.11) becomes

$$\rho_+(\underline{X}_0,k) = \mp(2ik) \iint_L \hat{n} \cdot \hat{X}_0 e^{-2ik\hat{X}_0 \cdot \underline{X}'} dS' \ . \qquad (A.12)$$

The domain of integration in (A.12) is only over the lit position L of the total surface ∂B . With the objective of obtaining a closed surface integral, we now write the analogous expression when the source-receiver point is reflected through the origin

[Figure (A.3)] . An analysis similar to that leading to (A.12) gives

$$\rho_-(-\underline{X}_0,k) = \pm(2ik) \iint_D \hat{n} \cdot \hat{X}_0 e^{-2ik\hat{X}_0 \cdot \underline{X}'} dS' \qquad (A.13)$$

Note that the lit and dark sides have been reversed; this assumption is valid only when the origin of coordinates is selected to lie within reasonable proximity to the target compared to the distance to the source-receiver point.

From (A.12) and (A.13), we now conclude that

$$\rho_+(\underline{X}_0,k) + \rho_-^*(-X_0,k) = \mp(2ik) \iint_{\partial B} \hat{n} \cdot \hat{X}_0 e^{-2ik\hat{X}_0 \cdot X'} dS',$$

and an application of the divergence theorem leads to

$$\frac{\rho_+(\underline{X}_0,k) + \rho_-^*(-\underline{X}_0,k)}{(2k)^2} = \pm \iiint_B e^{-2ik\hat{X}_0 \cdot \underline{X}'} dV' \ . \qquad (A.14)$$

Now introduce the characteristic function of the volume region occupied by B :

$$\Gamma(\underline{X}) = \begin{cases} 1 & \underline{X} \in B \\ 0 & \underline{X} \notin B \end{cases} ;$$

note that the Fourier transform of $\Gamma(\underline{X})$ is

$$\tilde{\Gamma}(\underline{\kappa}) = \underset{\substack{\text{all}\\\text{space}}}{\iiint} \Gamma(\underline{X}')e^{-i\underline{\kappa}\cdot\underline{X}'}dV' = \underset{B}{\iiint} e^{-i\underline{\kappa}\cdot\underline{X}'}dV' \ .$$

We may therefore rewrite (A.14) as

$$\tilde{\Gamma}(\underline{\kappa}) = \frac{\rho_+(\underline{X}_0,\kappa) + \rho_-^*(-\underline{X}_0,\kappa)}{\kappa^2} \qquad \text{(A.15)}$$

where $$\underline{\kappa} = 2k\hat{X}_0$$

Equation (A.15) constitutes the basic

POFFIS identity relating the Fourier transform of the characteristic function $\Gamma(\underline{X})$ to the backscattered, far-field quantities $\rho_{\pm}(\underline{\kappa})$.

Appendix B.

In this section, we outline the analogous calculations leading to the three-dimensional version of (2.10). Let D again represent an aperture which is both band and aspect angles limited, as shown in Figure (B.1). Parametricly, D is represented by

$$\kappa_0 \leq \kappa \leq \kappa_1$$

$$\phi \in [\phi_0, \pi - \phi_0] \cup [\pi + \phi_0, 2\pi - \phi_0]$$

$$\Theta \in [\Theta_0, \pi - \Theta_0] \cup [\pi + \Theta_0, 2\pi - \Theta_0]$$

where ϕ and Θ are the polar and azimuthal angles of $\hat{\kappa}$, respectively: $\hat{\kappa} = (\mathrm{Cos}\phi\mathrm{Sin}\Theta, \mathrm{Sin}\phi\mathrm{Sin}\Theta, \mathrm{Cos}\Theta)$. A separation of the magnitude and angular portions of the $\underline{\kappa}$-integration in (2.3) leads to

$$H(\underline{X},\hat{\xi}) = \left(\frac{1}{2\pi}\right)^3 \int_{\kappa_0}^{\kappa_1} \kappa^2 d\kappa \int_{\partial B} d\underline{\sigma}\hat{n}(\underline{\sigma}) \cdot \hat{\xi}$$

$$\iint_D e^{i\kappa\hat{\kappa}(\phi,\Theta) \cdot (\underline{X} - \underline{X}'(\underline{\sigma}))} \mathrm{Sin}\Theta \, d\phi d\Theta \qquad (B.1)$$

Choosing

$$\Phi = \hat{\kappa}(\phi,\Theta) \cdot (\underline{X} - \underline{X}'(\underline{\sigma})),$$

the stationary phase conditions become

$$\frac{\partial\Phi}{\partial\Theta} = \hat{\tau}_\Theta \cdot (\underline{X} - \underline{X}'(\underline{\sigma})) = 0 \ , \quad \hat{\tau}_\Theta = \frac{\partial\hat{\kappa}}{\partial\Theta} \qquad (B.2)$$

$$\frac{\partial\Phi}{\partial\phi} = \mathrm{Sin}\Theta \, \hat{\tau}_\phi \cdot (\underline{X} - \underline{X}'(\underline{\sigma})) = 0 \qquad (B.3)$$

$$\frac{\partial \Phi}{\partial \sigma_1} = \hat{\kappa}(\phi,\theta) \cdot \frac{d\underline{X}'(\underline{\sigma})}{d\sigma_1} = 0 \tag{B.4}$$

$$\frac{\partial \Phi}{\partial \sigma_2} = \hat{\kappa}(\phi,\theta) \cdot \frac{d\underline{X}'(\underline{\sigma})}{d\sigma_2} = 0 \tag{B.5}$$

Conditions (B.1) - (B.5) imply that the unit vector $\hat{\kappa}$ lies in the tangent plane to ∂B. A point of stationarity in (σ_1,σ_2) then occurs where $\underline{X} - \underline{X}'(\sigma_1,\sigma_2)$ lies along the normal line to ∂B. A lengthy calculation then leads to

$$H(\underline{X},\hat{\xi}) \sim \frac{1}{\pi} \frac{\hat{\xi} \cdot \hat{n}\ \mathrm{Sin}K|\underline{X} - \underline{X}'|}{|\det(u|\underline{X} - \underline{X}'|F + G)|^{1/2}|\underline{X} - \underline{X}'|} \Bigg|_{\kappa = \kappa_0}^{\kappa = \kappa_1} \tag{B.6}$$

where

$$u = \begin{cases} +1 & \underline{X} \in B \\ -1 & \underline{X} \notin B \end{cases},$$

and F and G represent the first and second fundamental coefficients of ∂B. Again the target surface ∂B may be identified by the peaking of the $\mathrm{Sin}X/X$ function when $\kappa_1 > \kappa_0 >> 1$; this gives information only about the portions Σ of the surface ∂B that have normal directions coinciding with the set of directions contained in the $\underline{\kappa}$-space aperture D.

A calculation similar to that leading to (2.14) again leads to the conclusion that no information concerning ∂B is available outside of the Σ region.

References

1. Bojarski, N.N., 1967, "Three-dimensional electromagnetic short-pulse inverse scattering", Syracuse University Research Corporation, Syracuse, New York.

2. Lewis, R.M., 1969, "Physical optics inverse diffraction", IEEE Transactions in Antennas and Propagation, AP-17, 308-314.

3. Perry, W.L., 1974, "On the Bojarski-Lewis inverse scattering method", IEEE Transactions on Antennas and Propagation, AP-22, 6, 826-829.

4. Tabbara, W., 1973, "On an inverse scattering method", IEEE Transactions on Antennas and Propagation, AP-21, 245-247.

5. _____, 1975, "On the feasibility of an inverse scattering method", IEEE Transactions on Antennas and Propagation, AP-23, 446-448.

6. Rosenbaum-Raz, S., 1976, "On scatterer reconstruction from far-field data", IEEE Transactions on Antennas and Propagation, AP-24, 66-70.

7. Greenspan, D., and Werner, P., 1966, "A numerical method for the exterior Dirichlet problem for the reduced wave equation", Arch. Ration. Mech. Anal., 23, 288-316.

8. Bleistein, N. and Handelsman, R.A., 1975, Asymptotic Expansions of Integrals, Holt, Rinehart & Winston, Inc., New York.

9. Majda, A., "High frequency asymptotics for the scattering matrix and the inverse problem of acoustical scattering", to appear.

Wave-Number k	Exact F.T. of Charact. Function $\tilde{\Gamma}(\underline{\kappa}) = \frac{\pi J_1(2k)}{k}$	Physical Optics Approx. to $\tilde{\Gamma}(\underline{\kappa})$	Relative Error, %
5	0.02731	0.04292	36.35
10	0.02100	0.01865	12.59
20	0.01980	0.01998	.92
30	0.00488	0.00509	4.12
40	-0.00440	-0.00438	.49
50	-0.00485	-0.00491	1.26
60	-0.00062	-0.00066	6.50
70	0.00253	0.00255	0.76
80	0.00209	0.00212	1.51

TABLE I

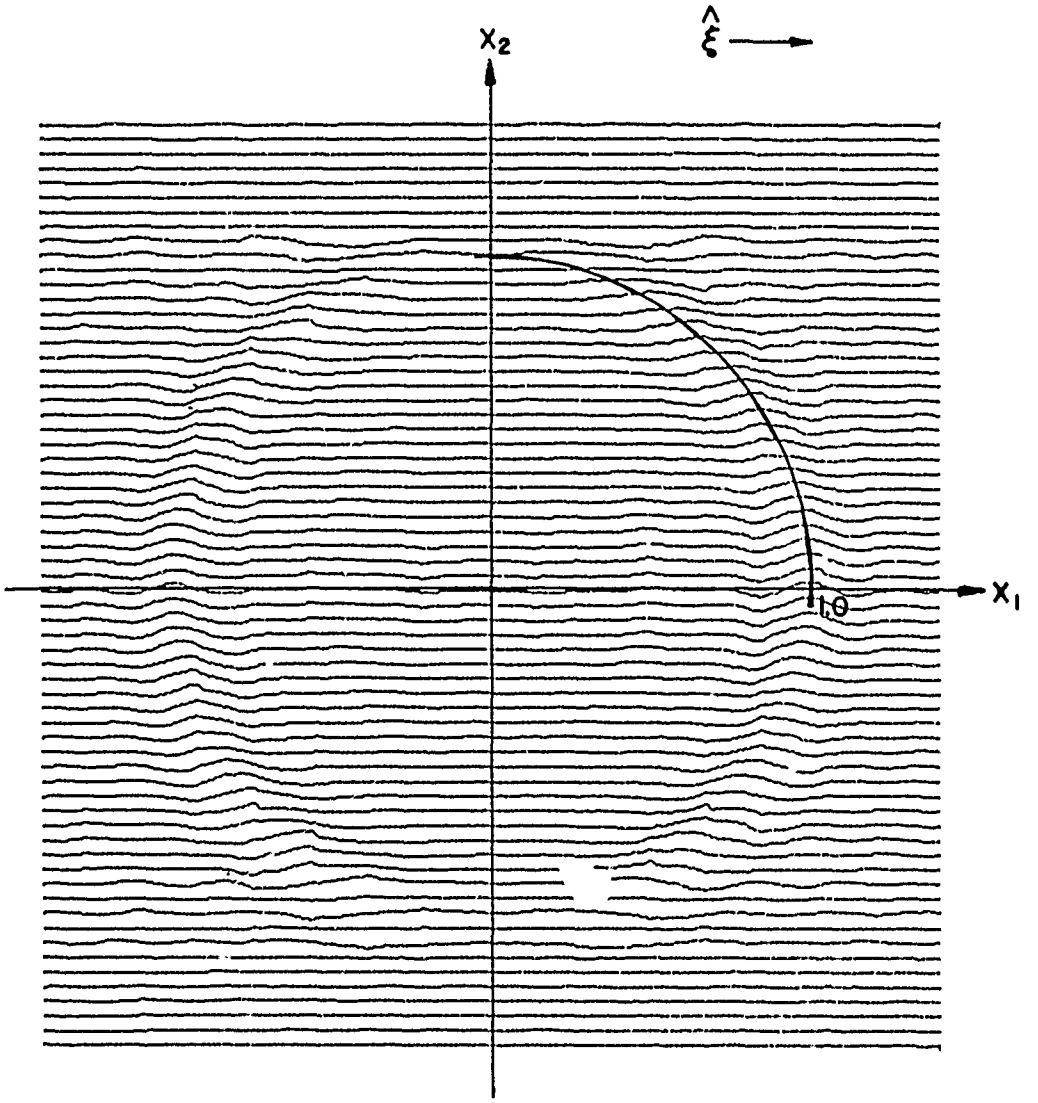

FIG. 2.1. $K_{MIN} = 5$, $K_{MAX} = 15$, RANGE = 25

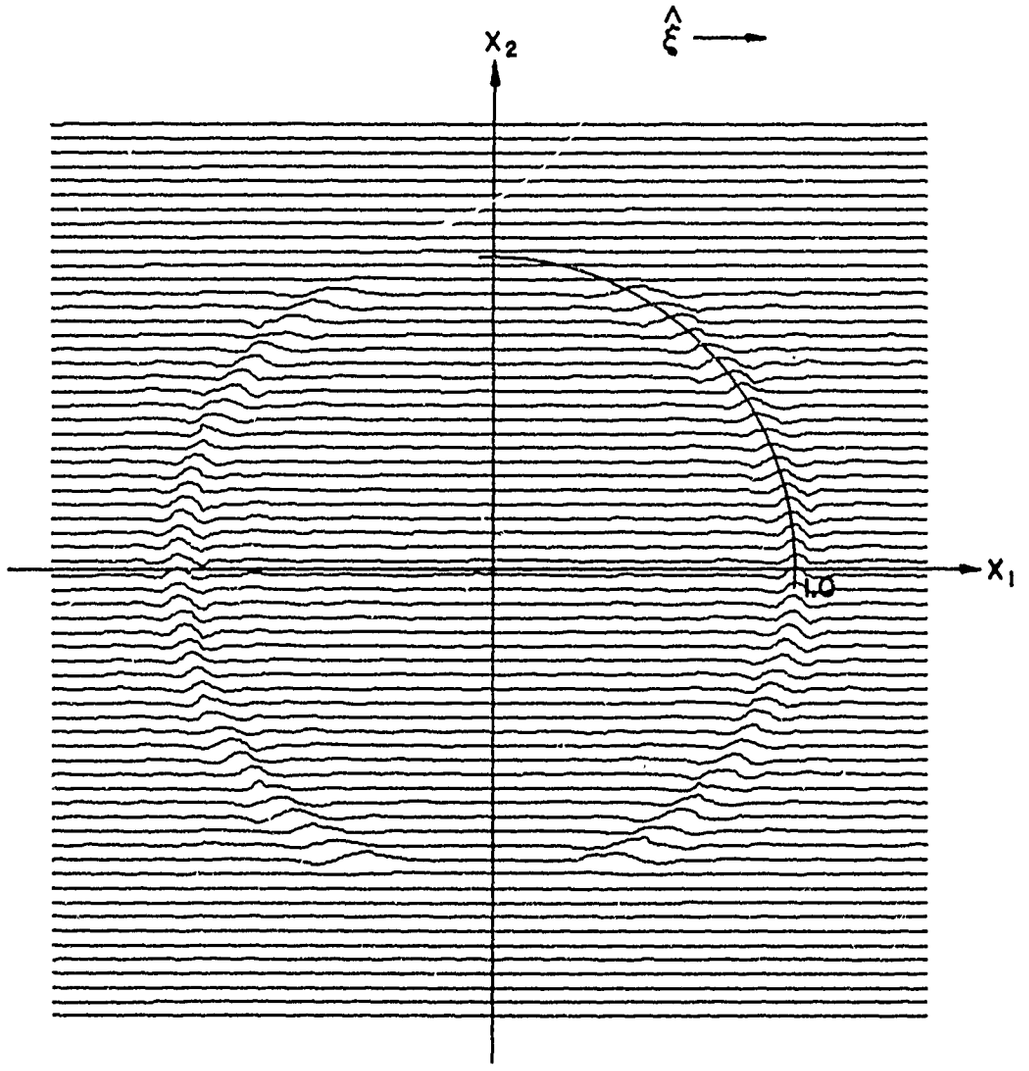

FIG.2.2. $K_{MIN} = 10$, $K_{MAX} = 30$, RANGE = 25

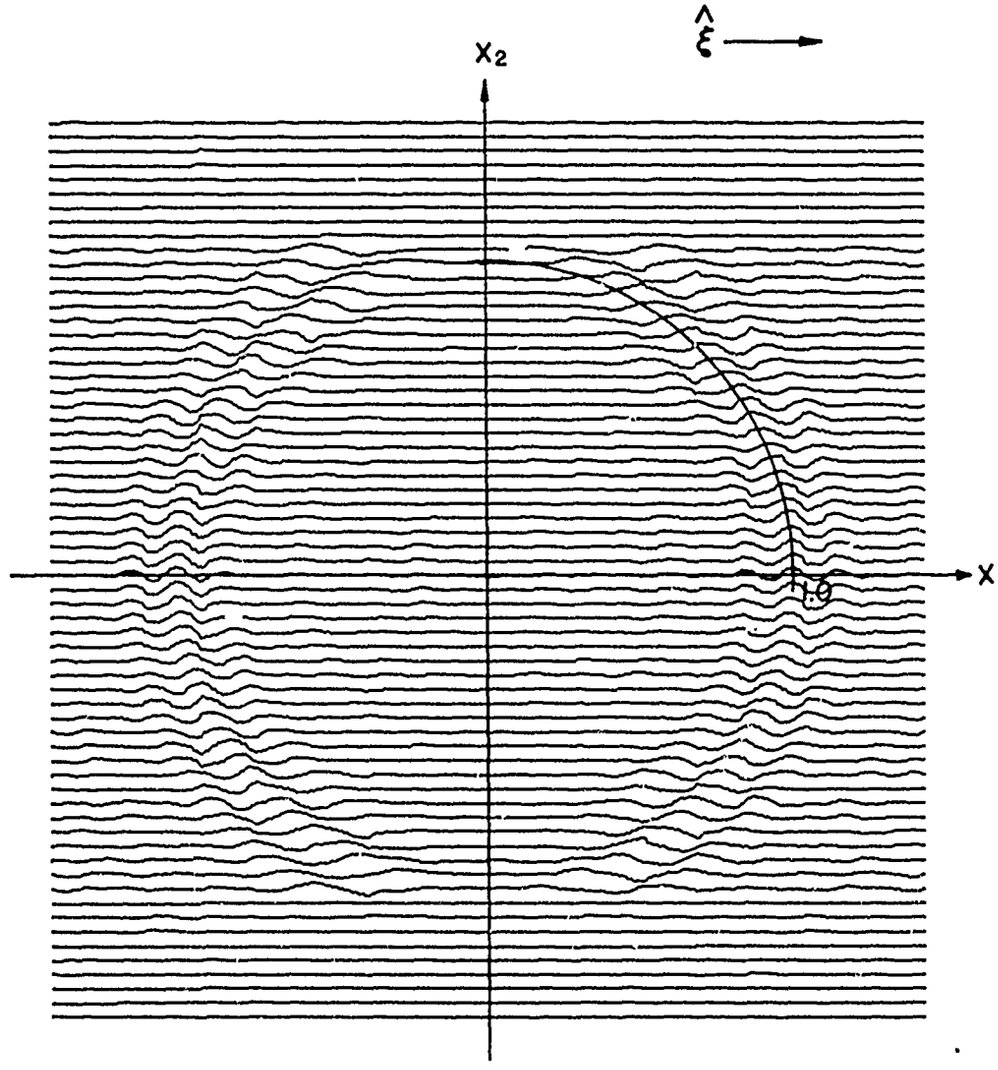

FIG. 2.3. $K_{MIN} = 15$, $K_{MAX} = 25$, RANGE = 25

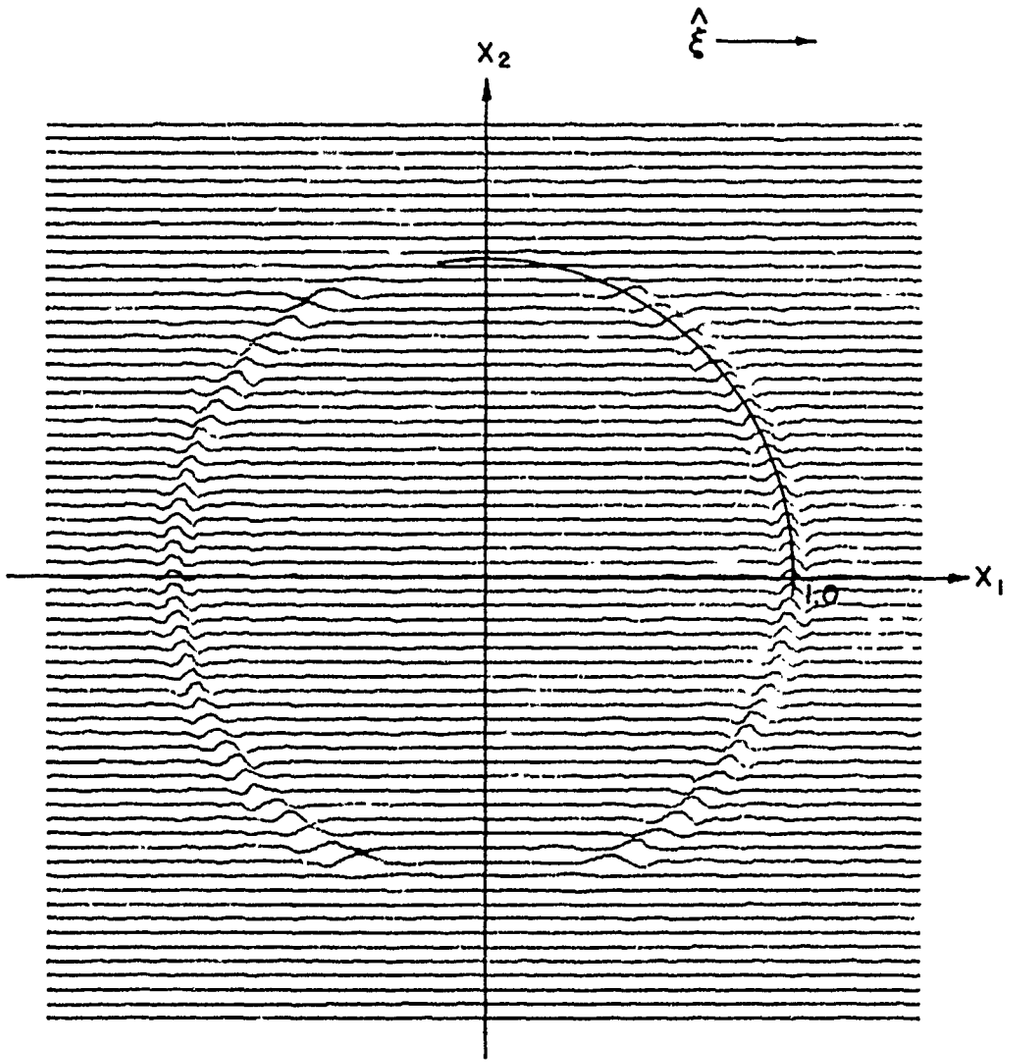

FIG. 2.4. $K_{MIN} = 15$, $K_{MAX} = 45$, RANGE = 25

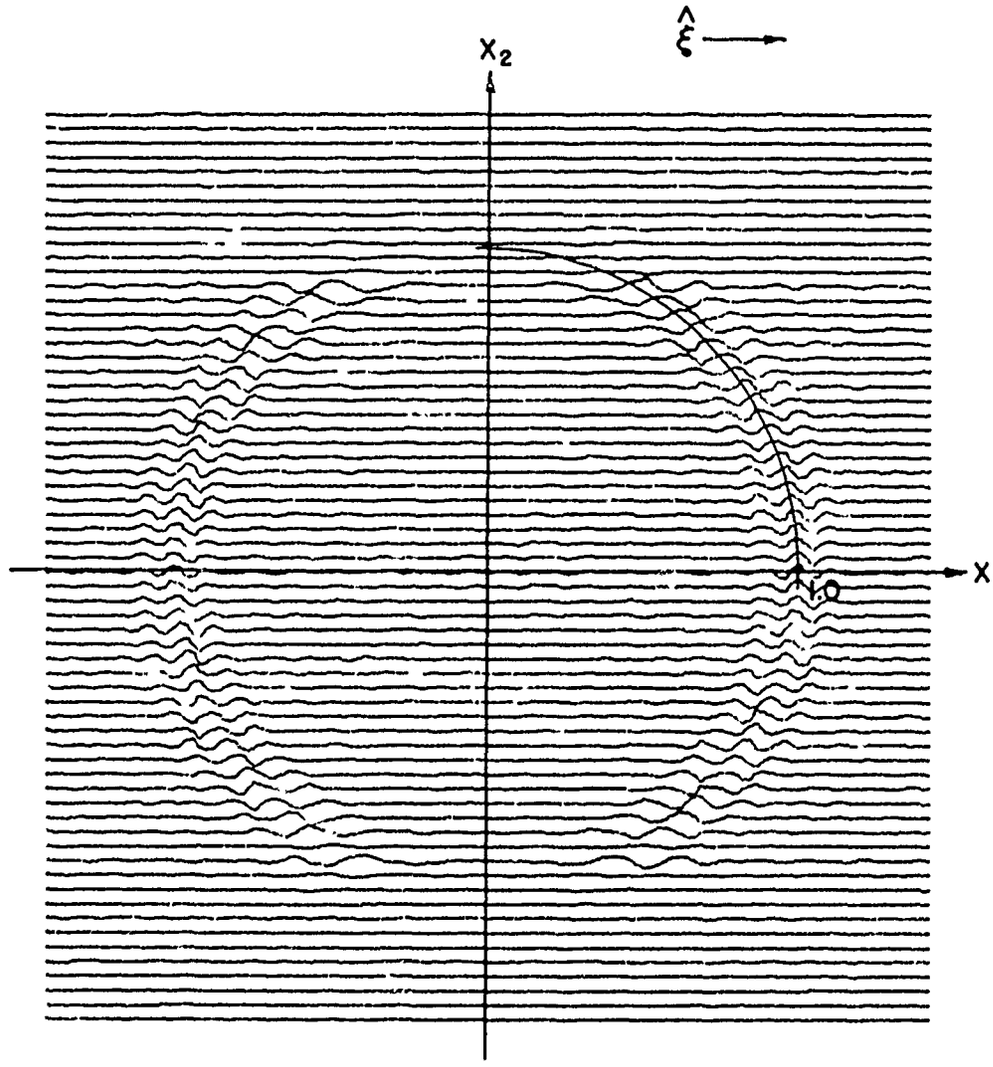

FIG. 2.5. $K_{MIN} = 22.5$, $K_{MAX} = 37.5$, RANGE = 25

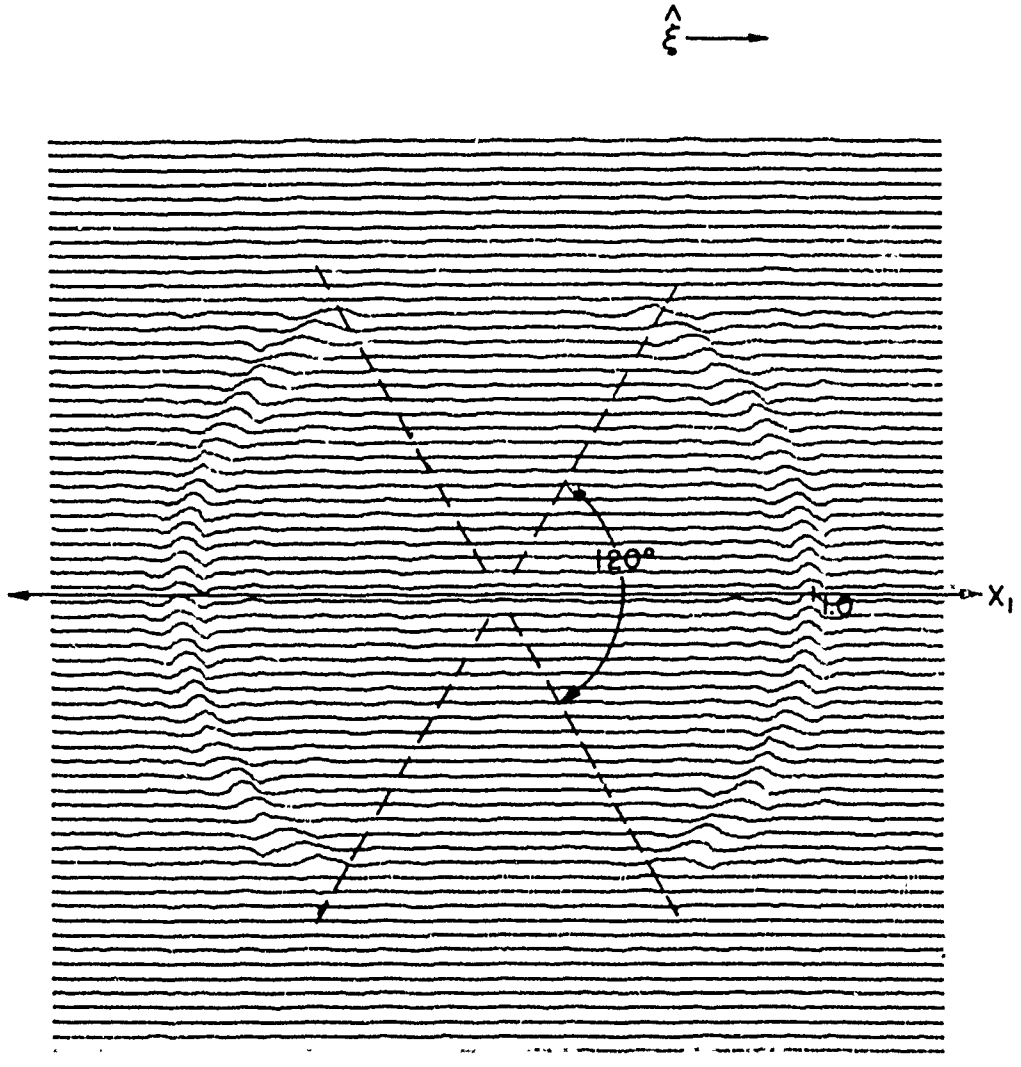

FIG. 2.6. $K_{MIN} = 10$, $K_{MAX} = 30$, RANGE = 25, ALPHA = 120°

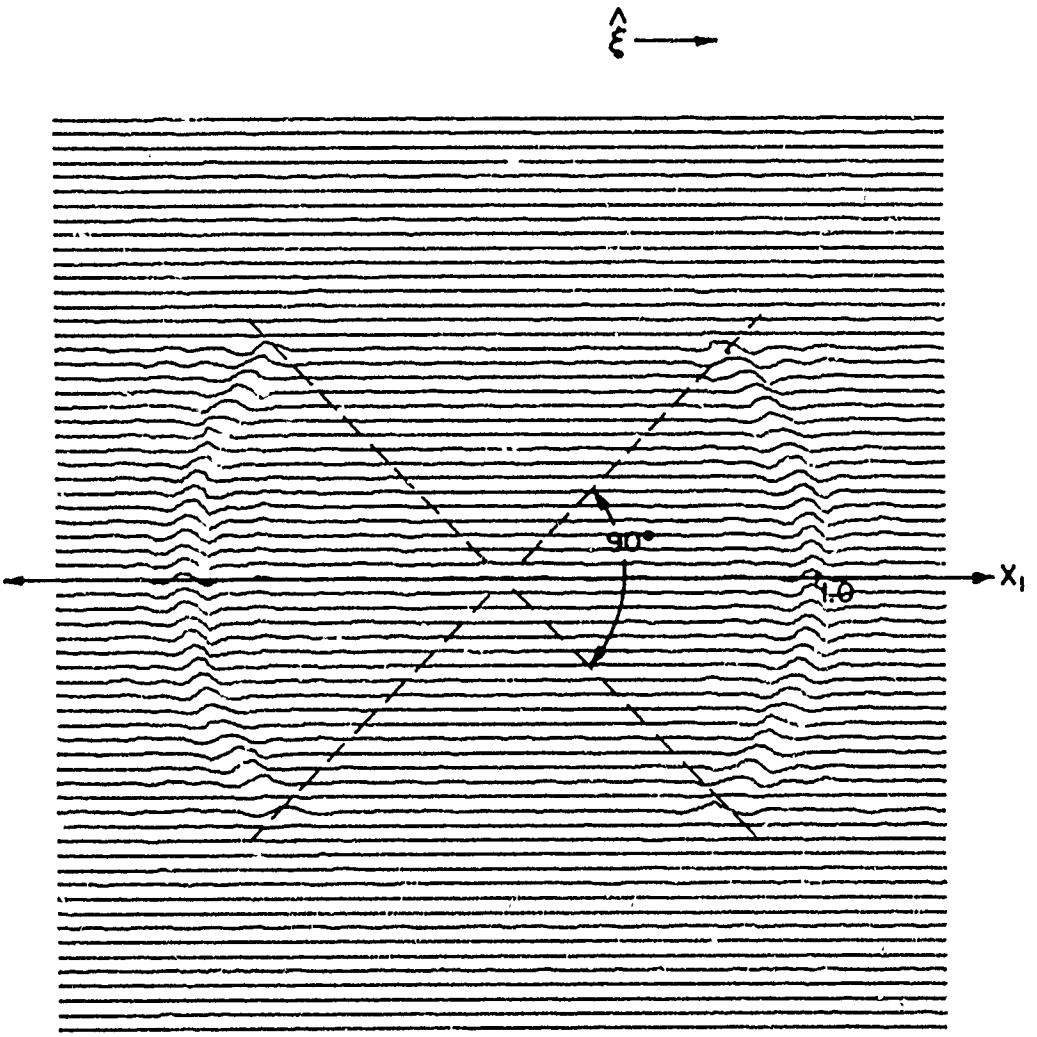

FIG. 2.7. $K_{MIN} = 10$, $K_{MAX} = 30$, RANGE = 28, ALPHA = 90°

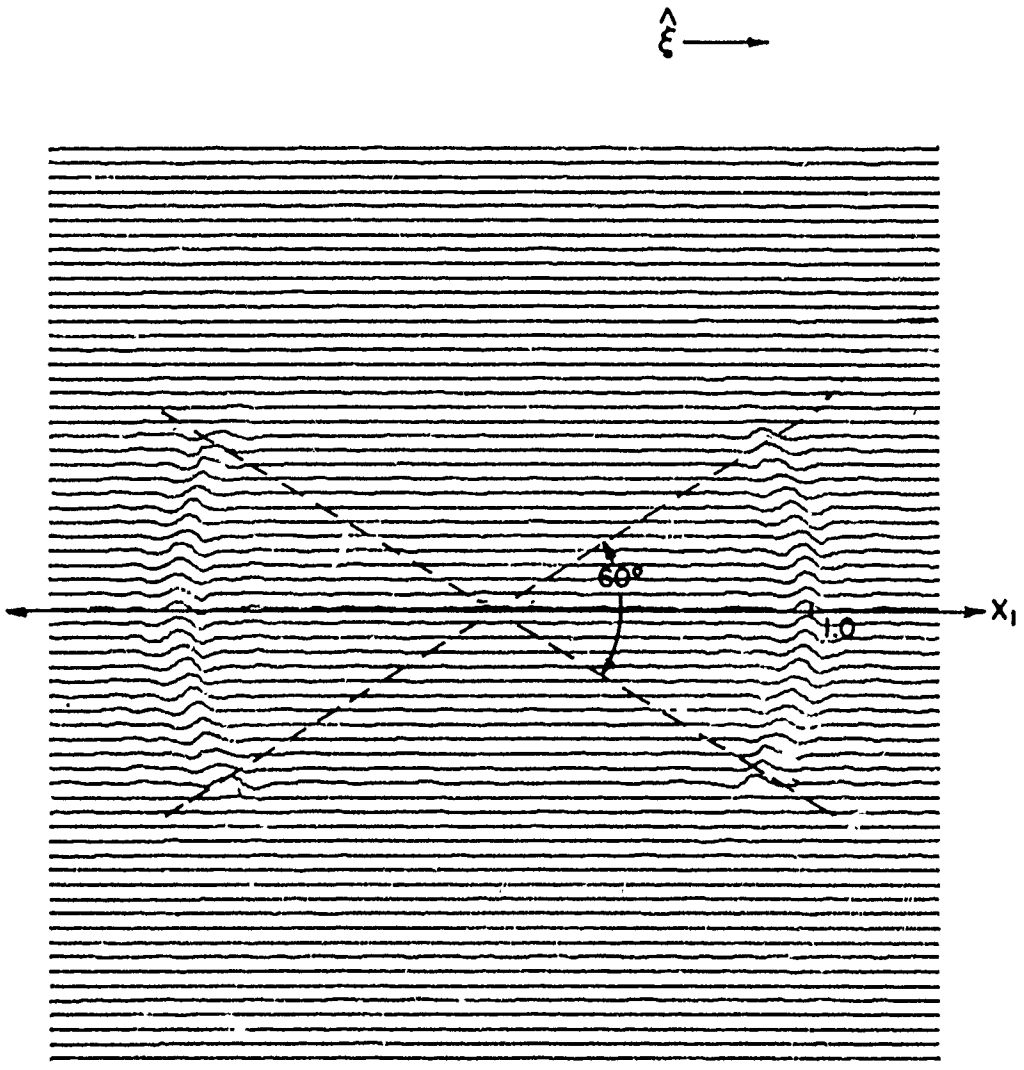

FIG. 2.8. $K_{MIN} = 10$, $K_{MAX} = 30$, RANGE = 25, ALPHA = 60°

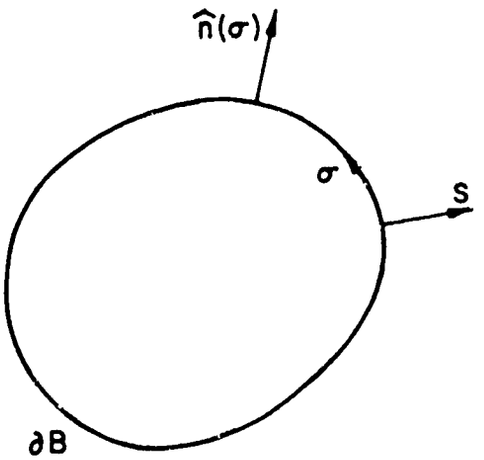

FIGURE 3.1. SHOWING TWO-DIMENSIONAL GEOMETRY.

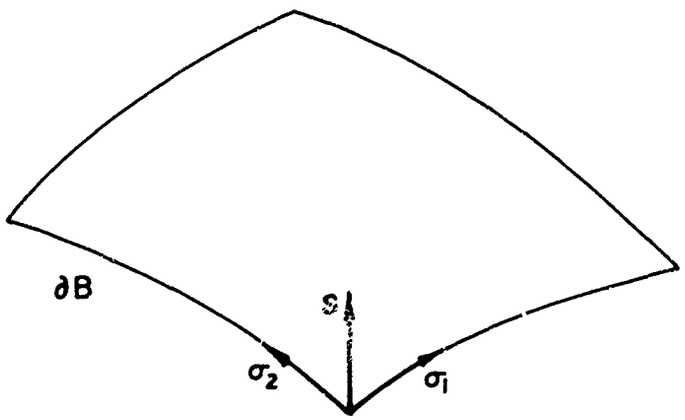

FIGURE 3.2 SHOWING THREE DIMENSIONAL GEOMETRY

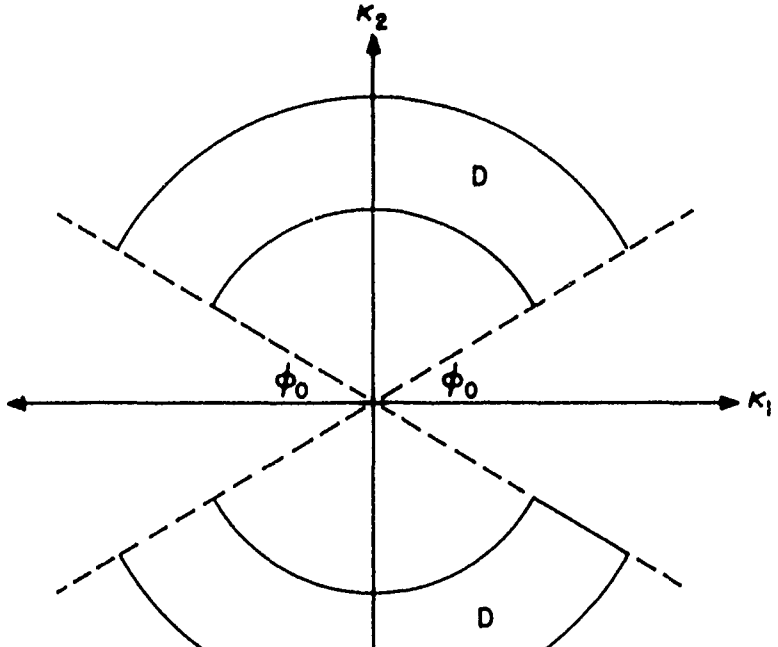

FIGURE 3.3 BAND AND ASPECT-ANGLES LIMITED APERTURE D IN $\underline{\kappa}$-SPACE

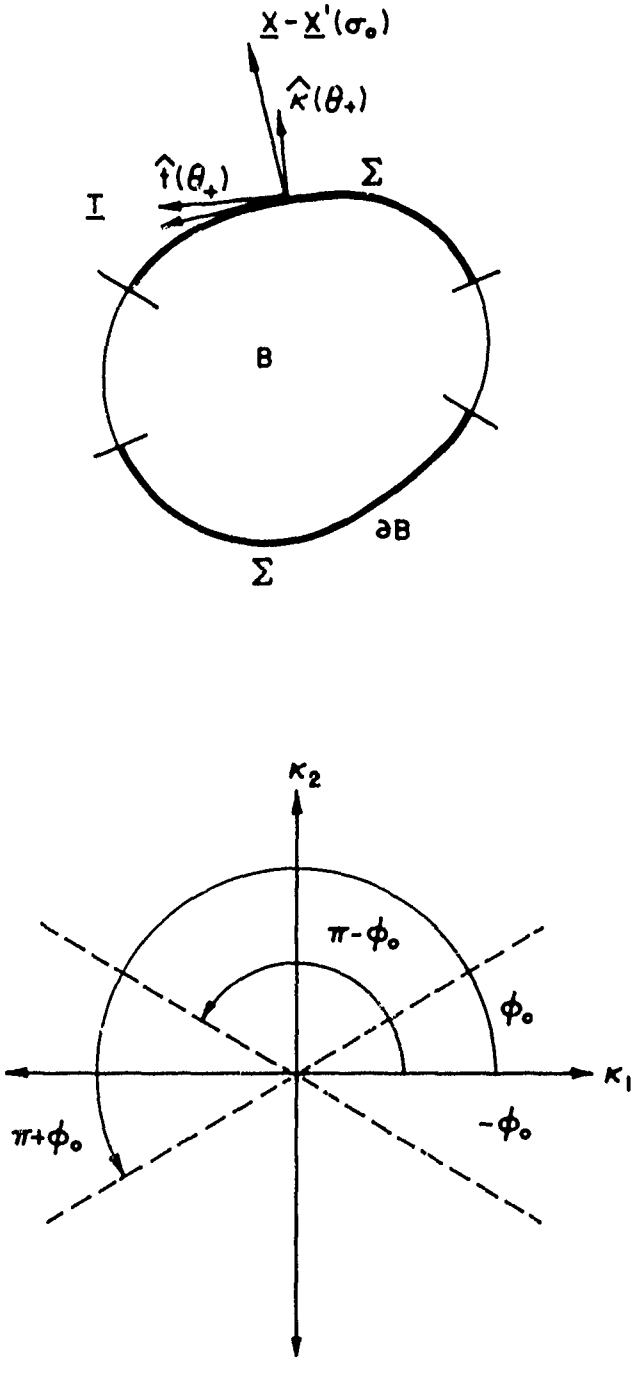

FIGURE 3.4. RELATIONSHIP BETWEEN Σ ON ∂B AND $\underline{\kappa}$-SPACE APERTURE OF VIEWING DIRECTIONS.

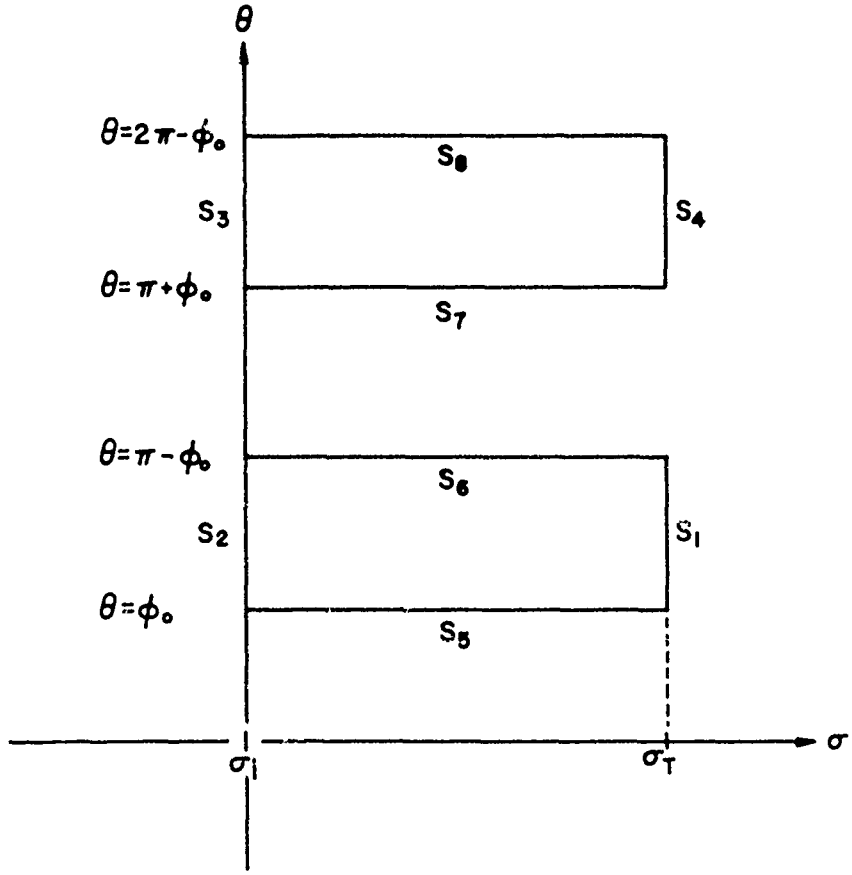

FIGURE 3.5. THE BOUNDARY $\partial(D,B)$ IN $\sigma-\theta$ SPACE.

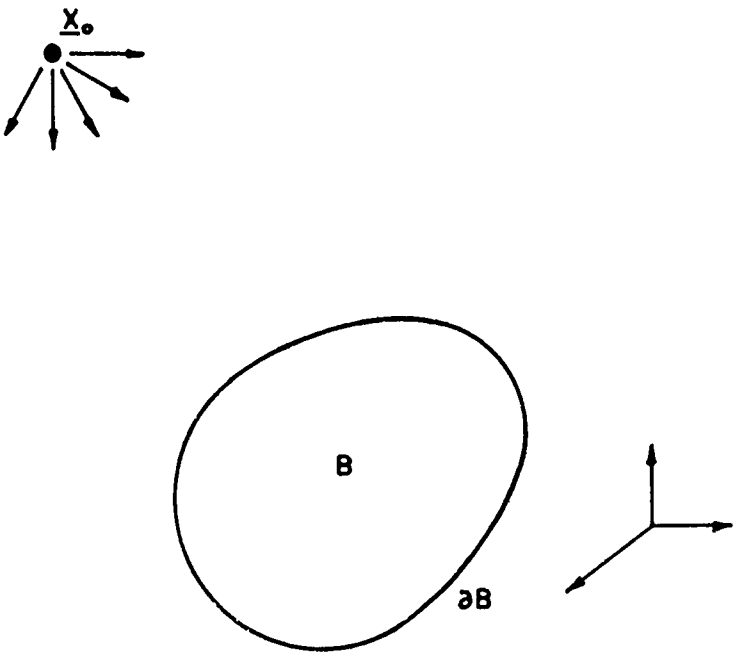

FIGURE A.I. SHOWING TARGET AND SOURCE-RECEIVER CONFIGURATIONS

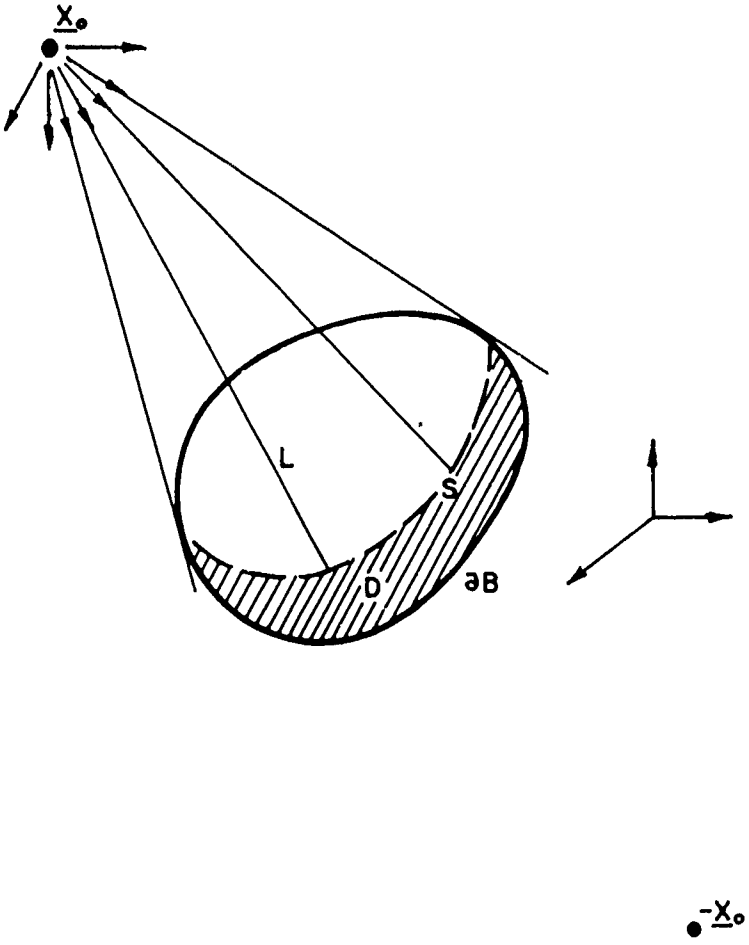

FIGURE A.2. SEPARATION OF TARGET SURFACE ∂B INTO LIT AND DARK SIDES

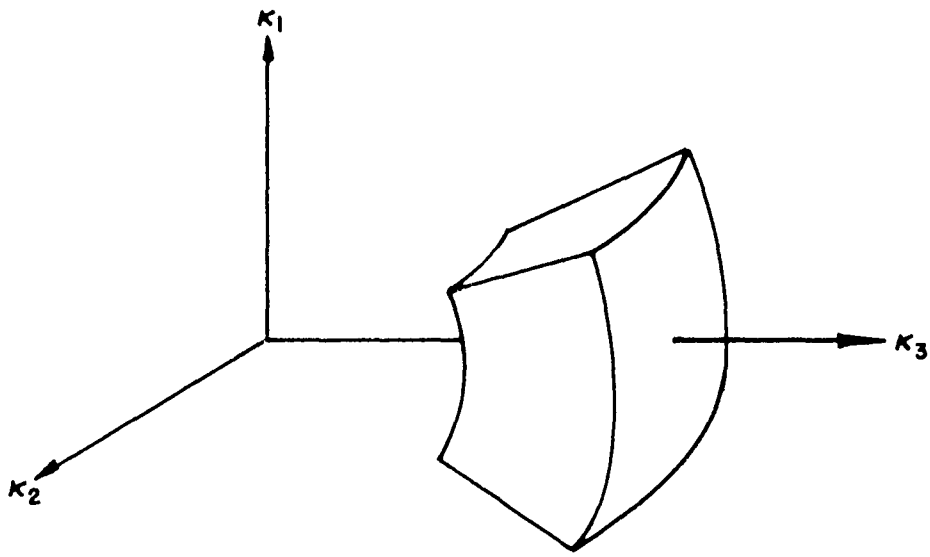

$$\kappa_0 \leq \kappa \leq \kappa_1$$

$$\theta_0 \leq \theta \leq \pi\ \theta_0 \text{ and } \pi + \theta_0 \leq \theta \leq 2\pi - \theta_0$$

$$\phi_0 \leq \phi \leq \pi\ \phi \text{ and } \pi + \phi_0 \leq \phi \leq 2\pi - \phi_0$$

FIGURE B.I. SHOWING $\underline{\kappa}$-SPACE APERTURE IN 3-DIMENSIONAL SPACE

UNCLASSIFIED

SECURITY CLASSIFICATION OF THIS PAGE (When Data Entered)

REPORT DOCUMENTATION PAGE

READ INSTRUCTIONS BEFORE COMPLETING FORM

1. REPORT NUMBER	2. GOVT ACCESSION NO.
3. RECIPIENT'S CATALOG NUMBER: MS-R-7704	
4. TITLE (and Subtitle): An Approach to the Limited Aperture Problem of Physical Optics Farfield Inverse Scattering	5. TYPE OF REPORT & PERIOD COVERED: Technical rept.
	6. PERFORMING ORG. REPORT NUMBER
7. AUTHOR(s): Robert D. Mager [redacted] Norman Bleistein	8. CONTRACT OR GRANT NUMBER(s): N0014-76-C-0039, N0014-76-C-0079
9. PERFORMING ORGANIZATION NAME AND ADDRESS: University of Denver, Denver Research Institute, Denver, Colorado 80208	10. PROGRAM ELEMENT, PROJECT, TASK AREA & WORK UNIT NUMBERS: NR-083-364 06-20-75; NR-041-434 06-10-75
11. CONTROLLING OFFICE NAME AND ADDRESS: Office of Naval Research, 800 North Quincy Street, Arlington, Virginia	12. REPORT DATE: 25 August 1976
	13. NUMBER OF PAGES: 28
14. MONITORING AGENCY NAME & ADDRESS(if different from Controlling Office): 48 pp.	15. SECURITY CLASS. (of this report): Unclassified
	15a. DECLASSIFICATION/DOWNGRADING SCHEDULE

16. DISTRIBUTION STATEMENT (of this Report)

This document has been approved for public release and sale; its distribution is unlimited.

17. DISTRIBUTION STATEMENT (of the abstract entered in Block 20, if different from Report)

N0014-76-C-0039, N0014-76-C-0079

18. SUPPLEMENTARY NOTES

19. KEY WORDS (Continue on reverse side if necessary and identify by block number)

Inverse Scattering
Physical Optics
Limited Aperture
Acoustics
Electromagnetics
Band-limiting
Characteristic Function

20. ABSTRACT (Continue on reverse side if necessary and identify by block number)

We ~~examine~~ the limited aperture problem of physical optics inverse scattering i.e., the problem of identifying a target from an analysys of band-limiting viewing apertures. ~~We show (given information from all directions) that~~ the target may be completely identified from an analysis of high frequency, band-limited data. If the directions of viewing angles are limited as well, it is shown that the target surface can be identified where the target normal lies within the range of viewing directions; outside of this range, no information

is examined

cont →

DD FORM 1 JAN 73 1473 EDITION OF 1 NOV 65 IS OBSOLETE S/N 0102-014-6601

UNCLASSIFIED

SECURITY CLASSIFICATION OF THIS PAGE (When Data Entered)

405 751

LB

is available. It is shown that this phenomenon is totally a feature of the Fourier transform of characteristic (one-zero) functions and independent of the inverse scattering formalism. Numerical examples are given for the case of a perfectly reflecting circular cylinder.